The Journal of Experimental Biology 213, 3378-3387

doi:10.1242/jeb.046367

Control of tumbling during the locust jump

David Cofer[1], Gennady Cymbalyuk[2], William J. Heitler[3] and Donald H. Edwards[2,*]

[1]Department of Biology, Georgia State University, Atlanta, GA 30303, USA, [2]Neuroscience Institute, Georgia State University, Atlanta, GA 30303, USA and [3]School of Biology, University of St Andrews, Fife KY16 9TS, UK

*Author for correspondence (dedwards@gsu.edu)

Accepted 26 June 2010

SUMMARY

Locust can jump precisely to a target, yet they can also tumble during the trajectory. We propose two mechanisms that would allow the locust to control tumbling during the jump. The first is that prior to the jump, locusts adjust the pitch of their body to move the center of mass closer to the intended thrust vector. The second is that contraction of the dorsolongitudinal muscles during the jump will produce torques that counter the torque produced by thrust. We found that locusts increased their take-off angle as the initial body pitch increased, and that little tumbling occurred for jumps that observed this relationship. Simulations of locust jumping demonstrated that a pitch *versus* take-off angle relationship that minimized tumbling in simulated jumps was similar to the relationship observed in live locusts. Locusts were strongly biased to pitch head-upward, and performed dorsiflexions far more often than ventral flexions. The direction and magnitude of tumbling could be controlled in simulations by adjusting the tension in the dorsolongitudinal muscles. These mechanisms allowed the simulations to match the data from the live animals. Control of tumbling was also found to influence the control of jump elevation. The bias to pitch head-upwards may have an evolutionary advantage when evading a predator and so make control of tumbling important for the locust.

Key words: locust, jumping, flight, tumbling, elevation, biomechanics, neuromechanical, simulation, model, invertebrate.

INTRODUCTION

Locusts can expertly control the trajectory and power of their jump to reach a specific target (Eriksson, 1980). However, high-speed video shows that they often tumble rapidly during the jump, sometimes making several complete revolutions throughout the jump trajectory (Pond, 1972). This makes the animal's orientation unpredictable during the ballistic phase of the jump and at the final destination, so that it is as likely to land on its back or head as on its belly. Because locusts are able to jump in both a predictable, controlled manner and in an erratic manner, it seems probable that they have mechanisms that enable them to control tumbling and that this ability may have evolutionary advantages.

The locust jump is composed of three phases, cocking, co-contraction and triggering. In the cocking phase, the tibia are fully flexed and a locking mechanism is engaged to prevent the tibia from extending prematurely (Heitler, 1974; Heitler and Burrows, 1977). During the co-contraction phase, the tibia extensor muscle contracts simultaneously with the flexor muscle and power is stored in the extensor apodeme, cuticle deformation, and the semi-lunar process at the femoro-tibial joint (Bennet-Clark, 1975; Burrows, 1995; Burrows and Morris, 2001; Heitler and Burrows, 1977). During the triggering phase, inhibitory neurons reduce the tension in the flexor muscle to allow the locking mechanism to disengage and release the stored energy to extend the tibia and produce the jump (Burrows, 1996; Heitler and Burrows, 1977; Pearson et al., 1980).

For a locust to jump accurately to a target, it must be able to control the length, the direction and the elevation of the jump. The length of the jump and the take-off velocity are governed by the amount of energy stored in the legs during co-contraction (Bennet-Clark, 1975; Sobel, 1990). The jump direction is determined by the orientation of the prothoracic legs as they rotate the body to point towards the target prior to the jump (Santer et al., 2005). The elevation of the jump is determined by the posture of the metathoracic legs. Thrust for the jump produced by each leg is applied along a straight line drawn from the distal end of the tibia through the proximal end of the femur (Sutton and Burrows, 2008); the angle made by this line and the horizontal (the 'beta angle') specifies the jump elevation (Fig. 1, red β). Control of elevation is separate from generation of the power for the jump, so these two variables can be controlled independently (Sutton and Burrows, 2008). These three mechanisms provide the locust with the means to aim its jump to a specific target and hit it accurately, but they do not address the issue of tumbling.

The posture of the two hind legs is usually identical before the jump so that the thrust vectors are in parallel. If the center of mass (COM) lies in the plane defined by the two thrust vectors, no forward (head-downward) or backward (head-upward) tumbling will occur. Although the COM is very close to this plane, it often does not lie in it (Albrecht, 1953; Alexander, 1968; Bennet-Clark, 1975). If the COM is below the plane of the thrust vectors, a negative torque will be generated that will cause the locust to tumble head-downward rapidly (Fig. 1A), and if the COM is above the thrust, then a positive torque will cause the body to rotate head-upwards (Fig. 1B).

We propose two mechanisms that the locust could use to control tumbling during a jump. First, it could adjust its posture before the jump to move the COM closer to the thrust vector. This would require the animal to change the elevation of the cephalothorax while leaving the orientations of the metathoracic legs unchanged. Second, it could generate an opposing torque during the jump impulse to counter the thrust torque. If, as is often the case, the COM is below the thrust vector, the COM could be brought upward by contraction of the dorsolongitudinal muscles between the thorax and abdomen (Baader, 1990). Contraction of these muscles would generate an offsetting torque to maintain the COM near the thrust vector (Fig. 1C). When the thrust was finished its torque would be removed,

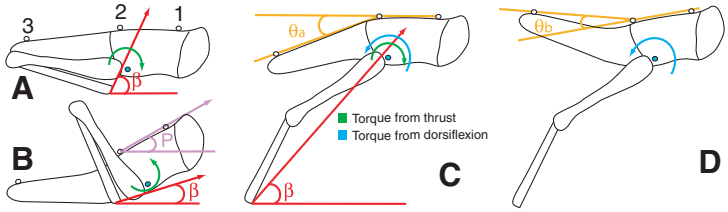

Fig. 1. The physics of tumbling. Jump elevation is determined by the beta angle (β), which is the angle between the horizontal and a line connecting the distal end of the tibia and the proximal end of the femur. The blue dot near the femur is the COM. The three beads along the dorsal thorax and the abdomen (numbered 1, 2 and 3) were used to measure pitch and abdominal flexion. Pitch (purple P) is the angle between the horizontal and a line segment through beads 1 and 2. Abdominal angle (θ) is the angle between a line through beads 1 and 2 and one through beads 2 and 3. Abdominal flexion is the difference in abdominal angle 6 ms after the feet leave the ground and the angle before they do so ($\theta_{flex}=\theta_b-\theta_a$). (A) When the beta angle is large and the initial pitch is small, the COM is below the thrust vector. This causes a negative torque and negative pitch velocities (clockwise arrow). (B) If the beta angle is small and the pitch is large, the COM is above the thrust vector. This causes positive torques and positive pitch velocities (counter-clockwise arrow). (C) The COM is below the thrust vector so a negative torque is generated that promotes a head-downward rotation (green arrow). Activation of the *dorsal longitudinal muscle* creates a counter-torque that promotes a head-upward rotation (blue arrow) that offsets the torque from thrust. (D) When the feet leave the ground, the thrust and the torque generated from it both end. The counter-torque from the abdominal muscle is unopposed and causes a visible flexion of the abdomen.

but the abdominal muscles would still be strongly activated. This would cause an abdominal flexion just after the feet left the ground (Fig. 1D). Activation of the ventral abdominal muscle near the end of the jump impulse would help to reduce the magnitude of the dorsiflexion and quickly bring the abdomen back into line with the body.

The locust's abdomen is used extensively during flight. Bending of the abdomen in the horizontal plane allows it to act as a type of rudder that is controlled by wind receptor hairs and proprioceptive information (Baader, 1990; Camhi, 1970b; Gettrup and Wilson, 1964). Abdominal curling is also used during flight to increase lift when it is near stalling speeds (Camhi, 1970a). If the abdomen plays such a role in the stabilization of flight, then it may also play a role in stabilization of the jump.

MATERIALS AND METHODS

Live animal analysis

Adult locusts, *Shistocerca americana* L., were obtained from a breeding colony at Agnes Scott College (Decatur, GA, USA), kept caged in small groups at 27°C under a 12 h:12 h L:D cycle, and fed fresh organic lettuce and a 2:1 mixture of fresh wheat germ and powdered milk. Individual locusts were removed from their cage and had their wings clipped off near the base to prevent flight during these tests. Lightweight white beads weighing 9 mg were glued onto the dorsal surface of the thorax and abdomen using superglue to provide position markers for motion analysis. One bead was placed near the head, another near the end of the thorax, and a third near the end of the abdomen (Fig. 1, beads 1, 2, 3). Three highly reflective 1 mm sequins were cut in half and glued onto the metathoracic leg. One was placed near the coxo-femoral (CF) joint, another at the midpoint of the femur, and a third near the femoro-tibial (FT) joint. After this treatment individuals were returned to their cage for a minimum of 4 h before being tested.

To perform tests, individuals were taken from the cage to a video-recording room and placed on a jumping platform. The platform contained a heating element that could adjust the local temperature and was covered by very fine sandpaper to provide the locust with a slip-free surface for jumping. A 25×30 cm rectangular yellow plane target was placed 30 cm from the platform, and jumps to the target were induced by either gently touching the abdomen with a hand-held wand or by raising the temperature of the platform. Animals were retrieved after the jump and returned to the platform for another attempt. Jumps were evoked at about 5 min intervals; individuals were returned to their cage after 10 jumps. Locust jumps were recorded at 500 frames s^{-1} and a resolution of 512×240 pixels by two Photron PIC R2 Fastcam video cameras (San Diego, CA, USA) with an exposure time of 0.5 ms.

Four of the seven animals tested (locusts 4–7) also had a 4.5 mm (diam.) steel ball (a 'BB' pellet) weighing 0.33 g glued onto the pronotum near the head in order to create an additional negative torque to extend the range of behaviors. A minimum of six jumps were performed with and without the weight for each animal. The weight was attached for the first set of jumps and removed for the second set for two animals, and removed for the first set and attached for the second set for the other two.

Only jumps that were perpendicular to the camera and in which the locust did not slip were analyzed. Analysis of the jump was performed using four video frames; the first at the beginning of the jump, the second just before the feet left the ground, the third 6 ms after the feet left the ground, and the final frame in which all beads and sequins were still visible. A custom Matlab application called MarkerCollector was used to analyze the four frames by manually selecting the center of each bead and sequin (Matlab R2007a, Mathworks Inc.). A ruler that was visible in each frame was used as a scale reference. The pitch of the locust was measured as the angle between the horizontal and the line formed between the beads 1 and 2 on the dorsal thorax (Fig. 1B). Take-off angle was the beta angle as the feet left the ground (Fig. 1C). Abdominal angle was the angle between the line formed by beads 1 and 2 along the thorax with the line formed by beads 2 and 3 along the abdomen (Fig. 1C,D). Abdominal flexion was defined as the change in the abdominal angle from just before they left the ground until 6 ms after the feet left the ground. An upward dorsiflexion of the abdomen was a positive value, and a downward ventral extension was negative. The take-off pitch velocity (TOPV) was the angular velocity while thrust was applied. It was calculated by finding the change in pitch between the beginning of the jump and when the feet left the ground. Positive velocity was head-upward. The tumbling pitch velocity (TUPV) was the angular velocity of the pitch after thrust was over. It was calculated by finding the difference between the pitch at the time the feet left the ground and at the time of the last frame that was analyzed, divided by the time between those frames.

Center of mass location

To determine the COM of a locust, an animal was placed alive in a refrigerator at 4°C for 2 h to anesthetize and immobilize it, weighed

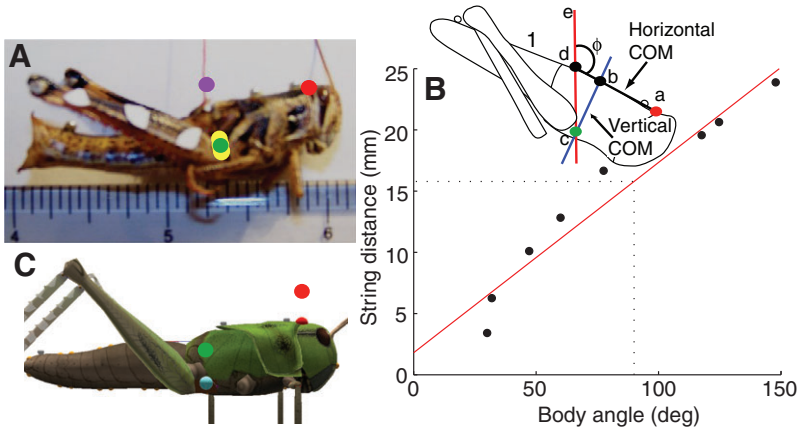

Fig. 2. Determination of COM. (A) Photograph of the frozen locust with a red thread attached to wax on the dorsal surface against an imperial and metric ruler. Only the one-sixteenth of an inch marks are visible in this picture. The reference point on the head is marked by a red dot; the measured COMs for different body angles (see B) are marked by yellow dots (an outlier is marked by the magenta dot), and their average is marked by a green dot. (B) A plot of the distance (in mm) of the attached string to the reference point *vs* the body angle (ϕ), and an illustration of the calculation of the COM (inset). The thread is attached vertically at d, and the reference point is at a (red dot). The distance from d to a varied linearly with the angle (ϕ) of the body from the vertical (R^2=0.983, P=7.7e–5). The position of the horizontal COM, b, along the line a–d was read from the regression line for an angle ϕ of 90 deg (dotted line in plot). The vertical COM (c, cyan dot) was determined by finding the intersection of a line extending the thread attachment (e–d) with a line (b–c) through the horizontal COM (b) perpendicular to a–b. (C) Image of the virtual *locust* with the position of the *COM* marked as a green dot.

and then killed by placing it in a freezer at –14°C overnight, and then reweighed in the morning, with no detectable difference in weight. Melted wax was placed on the dorsal surface of the thorax or abdomen and one end of a silk thread was embedded in the wax. The frozen locust was suspended by the thread from a pole and photographed with an 8 megapixel Kodak Z812IS camera (Fig. 2A). A ruler was visible in the plane of the locust to provide a distance calibration for the photographs. The wax attachment was moved in steps from the tip of the pronotum to the abdomen, the animal was re-suspended at each step, and a picture was taken. At each position the orientation of the locust changed based on the location of the COM relative to the attachment point. MarkerCollector was used to manually select data points for each image. The tip of the pronotum was chosen as a reference because it narrowed to a well-defined point and was clearly visible in all images.

The distance from the reference point to the thread attachment was measured (Fig. 2B inset, line a–d), along with the angle made between the dorsal surface of the thorax and the vertical thread attachment (Fig. 2B, angle ϕ). Attachment distances were measured and a linear regression was used to determine the distance along the dorsal surface from the reference where the body angle was 90 deg. This was the horizontal position of the COM. The vertical COM position was determined by placing a vertical line at the horizontal COM location and rotating it to match the body angle for each image (Fig. 2B, blue line b–c). The intersection of that line and the vertical line made by the string attachment (Fig. 2B, red line e–c) was the site of the COM (Fig. 2B, green dot at c). The vertical distance was measured between this point and the line used for the horizontal COM (Fig. 2B, blue line b–c). The average of that point for all images was used as the vertical position of the COM. Any data points that were more than 1.5 times the inter-quartile range were excluded from the analysis. Once the COM measurement was completed, the locust legs were removed and each body piece was measured, weighed, and photographed for use in the simulation.

Neuromechanical simulation

To distinguish between the model and its parts and the locust and its parts in the following account, the names of the model parts and behaviors are in italics and those of the corresponding locust body parts and behaviors are in normal font.

A neuromechanical simulation of one of the locusts was built using the software AnimatLab. AnimatLab is an open-source, freely available, Windows®-based software program in which models of the body and nervous system of any jointed animal can be assembled and tested for their effects on the model's behavior in a simulated physical world (www.AnimatLab.com) (Cofer et al., 2010a).

The body model and *neural circuit* that mediates the *jump* are shown in Fig. 3; details of both have been described previously (Cofer et al., 2010b). That model was used here with only a few modifications. Specifically, the sizes, masses of the *body parts*, and *COM* were altered to match the corresponding measurements of a single locust used in the high speed video analysis. The total body length of this animal was 50 mm with a mass of 2.4 g. The *abdomen* and *thorax* of the *locust body* each contained an internal mass whose position and density could be adjusted to equal the measured mass of the real body part and the COM of the body. The *locust COM* was set by pinning the *locust* in place (in simulation) and allowing it to rotate on a hinge joint. The densities and positions of the internal masses were adjusted to have the *locust* balance both horizontally and vertically at the measured COM location.

Hill-based muscle models were used to create *dorsal* and *ventral longitudinal muscles* between the *abdomen* and *thorax* (Albrecht, 1953), and the hinge joint connecting those two parts was set to allow a motion from 45 deg (dorsiflexion) to –45 deg (ventral flexion) (Hill, 1970; Shadmehr and Wise, 2005). We chose to use single dorsal and ventral longitudinal muscles in only the first abdominal segment in an attempt to reduce the overall complexity of the simulation. These *muscles* had the following properties: B (dashpot constant)=5 N s m^{-1}, K_{se} (serial spring constant)=20 N m^{-1}, K_{pe} (parallel spring constant)=1, and the maximum tension=1 N. The length–tension curve of each was set to be maximum at its resting length and to decrease as the *muscle* shortened. A non-spiking *neural compartment* was used to represent the common electrical properties of the *muscle membrane*. The *muscles* were stimulated directly by a depolarizing applied current ramp that was applied to the *muscle membrane* starting 24 ms before the onset of the *jump*. The response

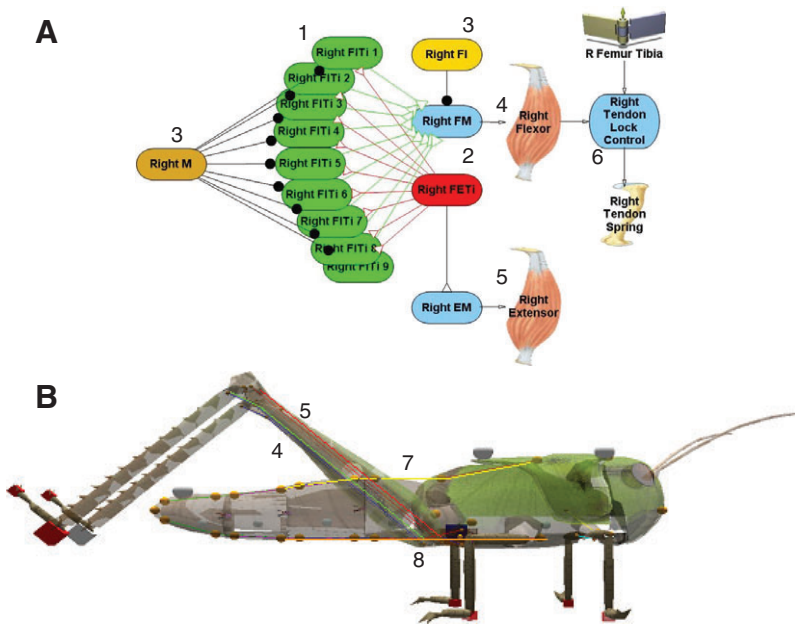

Fig. 3. The locust model. (A) The neural circuit for the jump (adapted from Cofer et al., 2010b). (1) *Flexor tibaei* (*FITI*) *motor neurons*; (2) *fast extensor tibiae* (*FETi*) *motor neuron*; (3) *inhibitory M* and *FI neurons*; (4) *flexor tibialis muscle*; (5) *extensor tibialis muscle*; (6) tendon lock. (B) The *locust* model with the *flexor* and *extensor muscles* labeled as in A; the *dorsal longitudinal muscle* (7) and *ventral longitudinal muscle* (8) extend between the *thorax* and *abdomen*. Elements of the model have been made transparent to reveal the muscles. Sequins are shown along the *dorsal thoracic-abdominal surface*. Cubes on the *tarsi* of each *leg* are zero-mass contact detectors; small gold-colored spheres are *muscle* attachment points.

of the *neural compartment* of each *muscle* was proportional to the stimulus current, and the sigmoidal stimulus–tension curve transduced the *membrane voltage* of the *muscle* to a maximal *muscle* tension, which was then modified according to the *muscle* length–tension curve. See Cofer et al. (Cofer et al., 2010a) for a detailed explanation of *muscle* properties.

To compare tumbling in the simulated and real locusts, we placed virtual beads and sequins on the *locust* to enable the *body pitch*, the *thoracic–coxa angle*, *the coxa–femur angle*, and the *beta angle* to be measured in the same manner as the real animal. The posture of a locust depends on an interaction between these angles. Because the *beta, thoracic–coxal (TC) joint* and *initial pitch* angles interact to produce a particular posture, setting one value affected the others. To address this, we created a postural control feedback system to help set the angles close to the desired values. Only simulated jumps that began with a *beta angle* within 0.5 deg and an *initial pitch* within 0.15 deg of the desired values were analyzed. The model used for these simulations can be found at http://www.animatlab.com/locust.

Simulation jump procedure

The simulation of the jump began with the locust held 1.5 cm above the ground when it was released and allowed to fall to the ground. This drop served to vary the initial positions and angles of the *legs* and *body* from trial to trial. Once on the *ground*, the *CF joints* of the *metathoracic legs* were rotated to elevate the legs 30 deg from horizontal to allow the *tibias* to flex fully without interference from the *ground*. Once the *tibias* were fully flexed, a *tendon lock* in each *leg* was engaged that held the *tibias* in position during the co-contraction phase. The *TC joints* were then moved to the user-defined angle, while the postural control system rotated the *CF joints* of the *front* and *rear legs* to attain the user-specified *beta* and *initial pitch angles*. All *leg* joints except the *FT* joint of *rear legs* were then locked or controlled until the beginning of the *jump*, which was defined as when the *tendon lock* system disengaged (Heitler, 1974). After the jump began, all *joints* were allowed to move freely.

A dorsiflexion of the *abdominal–thoracic joint* was evoked by applying a stimulus current to the *neural compartment* that represented the *muscle membrane*. The stimulus depolarized the *dorsal longitudinal muscle* and so increased its tension. A single jump from the high-speed video recordings provided the model for the simulated jumps. The beta and pitch angles of the locust at the beginning of that recorded jump were 29 deg and 1.72 deg, respectively; these values were in the middle of the range of angles recorded during the 22 jumps made by this animal (beta: 8.7 deg to

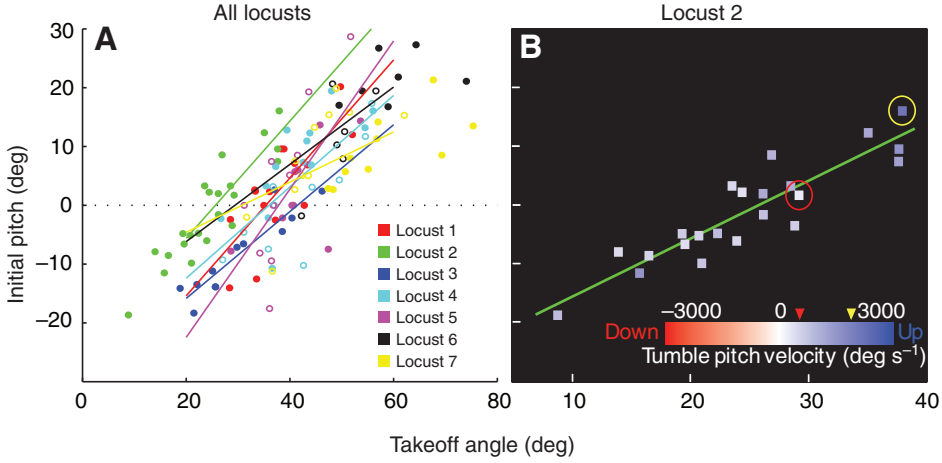

Fig. 4. Linear relationship between initial pitch and take-off angle. (A) Plots of initial pitch *vs* take-off angle for all jumps of seven locusts. Open circles represent jumps with weights attached and closed circles represent those with no weights. Regression lines for each individual locust are shown in different colors; the correlation coefficients and significance are given in Table 1. (B) Relationships of initial pitch, take-off angle and tumbling pitch velocity (TUPV) for locust 2. Each jump was color coded based on the TUPV. The yellow- and red-circled points were the minimum (237 deg s^{-1}) and maximum (1577 deg s^{-1}) pitch velocities. All of the jumps had a positive tumbling velocity regardless of the initial pitch or take-off angle. The data point circled in red was analyzed in more detail using simulations.

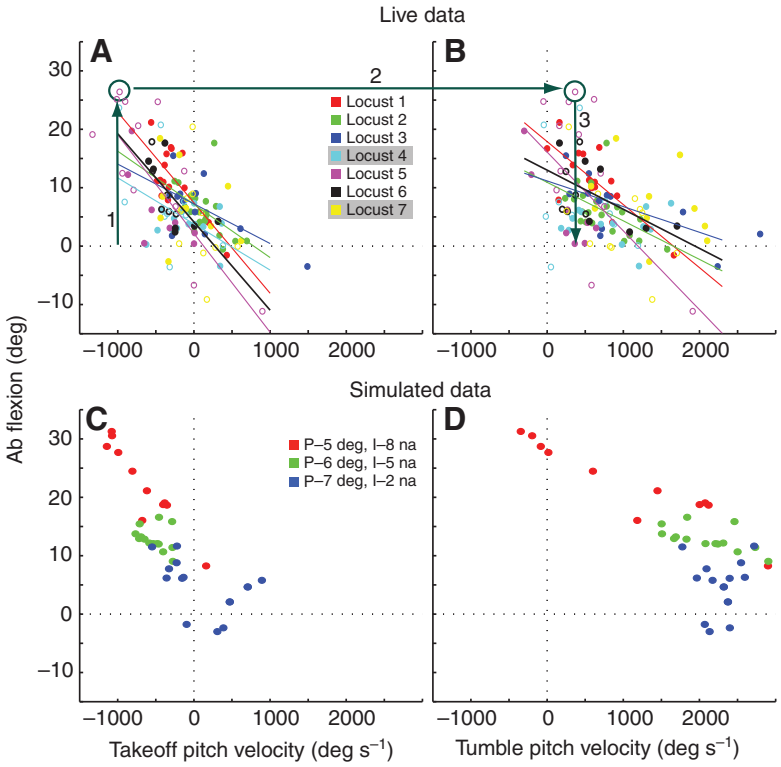

Fig. 5. Variation in abdominal flexion with pitch velocities for live (A,B) and simulated (C,D) jumps. (A,B) Abdominal flexion is plotted against take-off pitch velocity (TOPV; A) and tumbling pitch velocity (TUPV; B) for all jumps of seven locusts. Values for individual locusts are shown in different colors, with regression lines for those locusts for which the correlation was significant. Correlation coefficients and significance are given in Table 1. Locusts 4–7 performed jumps with and without weights attached to their pronotum. Open circles represent jumps with weights attached and closed circles represent those with no weights. (A) Dorsiflexion was greater for jumps with greater head-downward take-off pitch velocities (line 1). (B) TUPV was more positive than TOPV for nearly all jumps (lines 2, 3). (C,D) *Abdominal flexion* is plotted against *TOPV* (C) and *TUPV* (D) for all simulated jumps; points of the same color mark *jumps* from the same initial *pitch* and *dorsal longitudinal motor neuron* stimulus current. (C) Lower values for the initial pitch and larger stimulus currents evoked *jumps* with more negative *TOPV* values and larger abdominal flexion. (D) *TUPV* was more positive than *TOPV* for all *jumps*.

37.9 deg; pitch: –18.6 deg to 16.0 deg). These beta and pitch angles provided the values of the corresponding *beta* and *pitch* angles of the locust model for all simulated jumps in which these angles were not explicitly changed.

To determine the effect *beta angle* and *body pitch* on *tumbling behavior* of the model locust, the *beta angle* was varied between 20 deg and 40 deg in 2 deg increments, and the initial *body pitch* was varied between –4 deg and 16 deg in 2 deg steps. Simulations only tested a portion of the ranges found in live animals because at extreme values the simulated locust had trouble with *tarsal* slippage. *Take-off angle* was measured the same as for the data of the live locust but used the *CF joint* position instead of the sequin location. *Take-off and tumbling pitch velocities* were measured the same as for the live locust, but the final frame used to calculate *TUPV* was always 100 ms after the *feet* left the *ground*. Any simulation where the *locust* failed to jump further than 0.2 m or where the *tarsi* visibly slipped were excluded from the data sets.

RESULTS

Center of mass location

The horizontal location of the center of mass (COM) was determined to be 15.79±1.95 mm from the reference point on the back of the locust (Fig. 2A; Materials and methods). The vertical location was 9.47±0.88 mm from the horizontal COM. The projected locations of the COM for each data point are shown as yellow dots in Fig. 2A. There was a single outlier that was excluded from the analysis (Fig. 2A, magenta dot). It was produced when the locust was almost balanced and the two reference lines were nearly parallel. The projected location of the COM is shown as a green dot in Fig. 2A. The internal masses of the virtual *locust* were adjusted to approximate the COM calculated from the live animal. The location of the *COM* used in the simulations is shown as a green dot in Fig. 2C.

Tumbling during live jumps

We placed small weights on four of the locusts during half their jumps in an attempt to bias or extend the range of initial postures that were adopted. However, we found the locusts were able to adapt to the weights and showed very little difference in the resulting behavior (see Figs 4 and 5). Therefore, we combined all the data together for the resulting analysis.

There was a strong positive linear correlation between the initial body pitch immediately prior to the jump and the take-off angle for all the locusts (Fig. 4A; Table 1). Locusts adopted higher body pitches before jumps that had higher take-off angles, and *vice versa*. The take-off angle is determined by the beta angle of the legs adopted just prior to jumping (Sutton and Burrows, 2008). Although the beta angle was not measured for each of these jumps because the camera resolution was too low, these results indicate that the animal varied the body pitch with the beta angle before a jump. This would tend to move the COM upwards and closer to the thrust vector.

Locust number 2 was chosen as the model for the simulations. For this locust, like the others, there was a strong correlation between the take-off angle and initial body pitch for its jumps (Fig. 4B). Perhaps because of this correlation, there was no correlation between take-off angle (or initial pitch) and the angular velocity of the body after the animal left the ground (the tumbling pitch velocity or TUPV), which ranged from a minimum of 237 deg s^{-1} (Fig. 4B, red circle) to a maximum of 1577 deg s^{-1} (Fig. 4B, yellow circle), with an average of 744±335 deg s^{-1}. The locust produced jumps over a wide range of take-off angles and initial pitches, but TUPV remained positive and relatively small for all of them. All of the other locusts also displayed a positive TUPV, and there was a similar lack of correlation between take-off angle and TUPV for each individual's jumps.

Table 1. Correlation coefficients and significance for linear regressions shown in Fig. 4A and Fig. 5A,B of data from live locust jumps

		Fig. 4A: initial pitch *vs* take-off angle		Fig. 5A: Ab. flexion *vs* take-off pitch velocity		Fig. 5B: Ab. flexion *vs* tumble pitch velocity	
Animal	No. of jumps	R^2	*P*	R^2	*P*	R^2	*P*
1	15	0.598	7.2E–04	0.524	2.3E–03	0.582	9.5E–04
2	22	0.823	5.8E–09	0.261	1.5E–02	0.286	1.1E–02
3	12	0.852	1.8E–05	0.462	1.2E–03	0.486	1.2E–02
4	23	0.537	7.0E–05	0.228	2.1E–02	0.076	**2.0E–01**
5	21	0.580	9.5E–05	0.610	4.8E–05	0.312	1.0E–02
6	13	0.464	1.0E–02	0.464	1.0E–02	0.310	4.8E–02
7	20	0.375	3.2E–03	0.120	**1.2E–01**	0.084	**2.0E–01**
Combined	126	0.592	6.0E–26	0.615	1.9E–14	0.479	1.4E–08

Ab., abdominal.
R^2 is the correlation coefficient for the three plots in the figures, and *P* is the significance. Data that was not significant at the 0.05 level is in bold type, and their regression lines were excluded from Fig. 5A,B.

We found that in many of the jumps, that the locusts would flex the abdomen upwards. In six of the seven locusts tested, the amount of abdominal flexion measured at take-off (see Materials and methods) was significantly correlated with the pitch velocity at take-off (TOPV; Fig. 5A). The largest dorsiflexions occurred when initial tumbling was most strongly head-downward (Fig. 5A, line 1). The head-downward tumbling then slowed and reversed (Fig. 5A,B, lines 2 and 3) to become slow head-upward tumbling. This resulted in a small angular velocity (TUPV) after the thrust was finished (Fig. 5B, lines 2, 3). In five of these six locusts, abdominal flexion also correlated with the pitch velocity after leaving the ground (TUPV; Fig. 5B). The plots of abdominal flexion *vs* TUPV are roughly parallel to, and shifted right from, the corresponding plots of abdominal flexion *vs* TOPV, indicating that all abdominal flexions produced nearly the same increase in pitch velocity, from TOPV to TUPV (890±335 deg s^{-1}).

The change in pitch velocity (i.e. angular velocity) of the locust is an angular acceleration that must have been produced by a torque operating on the animal. We propose that this torque was the difference between the initial negative torque produced by the jump and the subsequent positive torque produced by the abdominal flexion. The constant increase in pitch velocity at all abdominal flexions suggests that the positive torques produced by the abdominal flexions always exceeded the initial negative torques by a similar amount. This result stresses the importance for locusts of avoiding head-downward tumbling and suggests a mechanism for how they do so.

Tumbling during simulated jumps

A single jump of locust 2 provided the parameter values used in the jump simulation (Fig. 4B, red circle; Fig. 6A). Locust 2 prepared for the jump with a small initial pitch of 1.72 deg and a beta angle of 29 deg (Fig. 6A1). As its tarsi left the ground, its body pitch increased by less than a degree with a TOPV (take-off pitch velocity) of 16.4 deg s^{-1} (Fig. 6A2), and 6 ms later a small abdominal flexion of 8.1 deg occurred (Fig. 6A3). Finally, the locust pitched head-upward with a small TUPV of 237 deg s^{-1} (Fig. 6A4).

For the simulated *jump*, the *pitch* and *beta angle* of the locust model were set by a feedback controller (see Materials and methods) to be close to the corresponding values, 1.72 deg and 29 deg, measured from the high-speed video of locust 2's jump. The *COM* was below the *thrust vector* (Fig. 6B1 inset), indicating that the *torque* on the *body* would be negative, causing the animal to pitch head-downward. Images from the high-speed video of the jump (Fig. 6A) were compared with snapshots of the virtual *locust jump* simulations (Fig. 6B,C). The *locust jump* began with an *initial pitch* and *beta angle* similar to the real animal (Fig. 6B1), but the behavior of the simulation quickly diverged. During *take-off*, the *body*

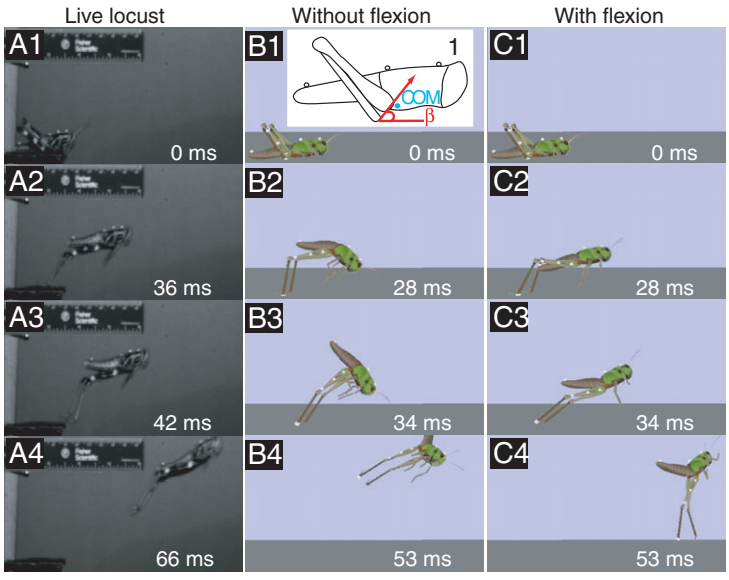

Fig. 6. Comparison of live and simulated *jumps* with and without *dorsiflexion*. (A1) Locust 2 just prior to jumping. The initial pitch is small (1.72 deg). (A2) Just before the locust's feet left the ground. The initial pitch remained steady throughout the jump (TOPV=16.4 deg s^{-1}). (A3) 6 ms after it's feet left the ground. A small dorsiflexion of the abdomen is visible. (A4) Final trackable frame of the jump. The locust has pitched up slowly. (B1) Simulated *locust* prior to *jumping* with no *dorsiflexion*. Initial conditions were set to attempt to recreate the jump of the live locust. (1) Inset shows the approximate location of the COM relative to the thrust vector for the simulated jump. (B2) *Locust* just before the *feet* left the ground. Unlike the live animal, *body pitch* of the simulated *locust* rapidly decreased (*TOPV*=–2260 deg s^{-1}). (B3) The *body* somersaulted in a head-downward *tumble* (clockwise) as the *legs* swung forward (counter clockwise). (B4) When the limits of the *thoracic–coxa joints* were reached, the angular opposing momenta of the *legs* and *thorax* largely cancelled their rotational movements. (C1) *Locust* prior to *jumping* with *dorsiflexion*. (C2) Initial *pitch* was very similar to the live locust and remained nearly constant throughout the *jump impulse* (*TOPV*=–2.59 deg s^{-1}). (C3) A *dorsiflexion* began immediately after the thrust was finished. (C4) The *locust* activated the *dorsal longitudinal muscle* and not the *ventral longitudinal muscle*, and so *dorsiflexion* reached a maximum and was maintained throughout the *jump*. The *tumbling* rate was positive (*TUPV*=365 deg s^{-1}).

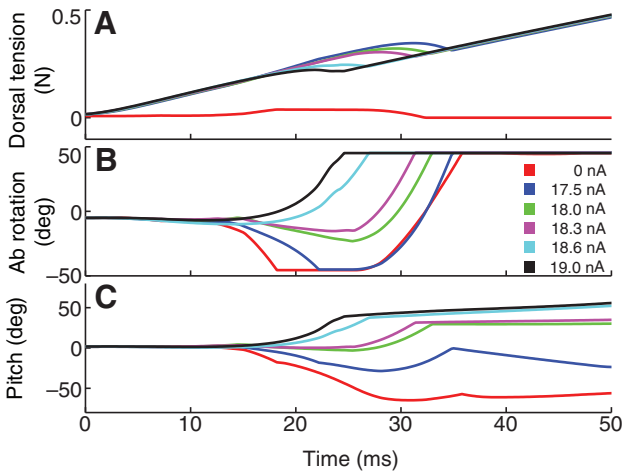

Fig. 7. Change in dorsal longitudinal muscle tension, abdominal flexion and body pitch during a jump. The amplitude of the stimulus current ramp applied to the *dorsal longitudinal muscle membrane* was absent, or varied between –17.5 and 19 nA for a series of simulated *jumps*. The ramp current was applied starting 24 ms before the jump began. Details are shown in Table 2. The chart time begins at the start of the jump when the tendon lock was released. The *dorsal longitudinal muscle* tension (A) increased continuously following the stimulus current, until *abdominal* flexion reduced it by reducing or reversing *abdominal* rotation (B) and the pitch of the *thorax* (C).

rotated rapidly downward and attained a *TOPV* of –2260 deg s^{-1} (Fig. 6B2). Rotation continued as the *locust* turned in a somersault (Fig. 6B3).

To determine whether the dorsiflexion observed during locust jumps could evoke sufficient counter torque to stop or reverse the direction of tumbling, a ramp stimulus current was applied to the *dorsolongitudinal muscle membrane* in the second simulation, beginning 24 ms before release of the *tendon lock*. The second *locust jump* began identically to the first (Fig. 6C1). However, the behavior during thrust application (Fig. 6C2) was much more similar to that of the live animal (Fig. 6A2) than to the simulated *jump* without *dorsiflexion*. Instead of the strongly negative *TOPV* seen in the absence of the *dorsiflexion* stimulus (Fig. 6B2), *TOPV* with the stimulus was reduced to –2.59 deg s^{-1}. Soon after the thrust ended and contraction of the *dorsolongitudinal muscle* persisted, a small *abdominal* flexion occurred (Fig. 6C3), and the *locust* had a positive *TUPV* of 365 deg s^{-1} (Fig. 6C4).

We found that *take-off and tumbling pitch velocities* could be controlled by varying the amount of tension in the *dorsal longitudinal muscle* during the *jump* impulse (Fig. 7A). The tension of the *muscle* was set by varying the amplitude of the stimulus current ramp applied to the *muscle membrane*. With no stimulus current, the *thoracic–abdominal joint* quickly flexed ventrally to its maximal value (Fig. 6B2 and Fig. 7B, red), while the *pitch* of the *thorax* also rapidly declined (Fig. 7C, red). With a stimulus current, *dorsal longitudinal muscle* (*DLM*) excitation enabled the *locust* to counter the negative torque. By varying the *muscle membrane* stimulus current amplitude, the *TOPV* could be controlled so that it varied between –1078 deg s^{-1} at 17.5 nA and +1337 deg s^{-1} at 19 nA (Fig. 7C; Table 2).

To explore the relationship between *pitch velocity*, *initial pitch*, *beta angle* and the effects of *DLM* activation, *jumps* were evoked with and without *DLM* activation, while the *initial pitch* and *beta angle* were systematically varied. The resulting *take-off pitch velocities* and *tumbling pitch velocities* of the simulated jumps are color-coded in plots of *initial pitch* against the *beta angle* in Fig. 8. When *dorsiflexion* was not activated, *jumps* in which the *TOPV* was close to zero appear in Fig. 8A as a narrow strip (white dots) flanked below (*jumps* with larger *beta angle* or smaller *initial pitch*) by head-downward *tumbling jumps* (pink and red dots) and above (smaller *beta angle* or larger *initial pitch*) by head-upward *tumbling jumps* (blue dots). Head-downward *tumbling* was reversed or eliminated for most jumps at greater initial pitches some milliseconds after *take-off* (Fig. 8B). For *jumps* at lower *initial pitches*, the head-downward *tumbling* rate decreased somewhat because the *thoracic–coxa joint* reached its limits and the opposing angular momenta of the *legs* and *thorax* largely cancelled their rotational movements.

The simulated *jumps* were repeated and a *dorsiflexion* was evoked during any *jump* that had a head-downward *TOPV* without *dorsiflexion*. For each of these jumps a *dorsiflexion* stimulus was chosen that caused the head-downward *TOPV* to be either eliminated or somewhat reversed (Fig. 8C). The *TOPV* for these points increased significantly from an average of –1682±1083 deg s^{-1} when there was no *dorsiflexion* to a value of –290±705 deg s^{-1} when *dorsiflexions* were used (P<1e–15). *Dorsiflexion* had a similar but more modest effect on all *TUPV* values, eliminating or reversing the direction of *tumbling*, particularly for *jumps* that began with a low initial *pitch* (Fig. 8D).

The simulated *jumps* were compared with the jumps recorded for locust 2 by superimposing the TUPV regression line of Fig. 4B (green line) onto the patterns of simulated *jumps* (Fig. 8A–D). The green line lies along the strip of simulated *jumps* for which minimal *tumbling*

Table 2. Comparison of live and simulated locust *jumps*

Jump type	Dorsi-flexion stimulus	Beta angle	Initial pitch	Take-off angle	TOPV	TUPV
Live locust	–	–	1.72	29	16.4	237
Simulated	0.0	29.1	1.79	50	–2260	280
Simulated	17.5	28.5	1.54	41	–1078	–796
Simulated	18.0	28.5	1.54	38	–158	529
Simulated	18.3	28.5	1.54	35	–2.59	365
Simulated	18.6	29.4	1.82	29	767	613
Simulated	19.0	28.5	1.54	25	1337	455

Characteristics of the jump of live locust 2 on which the simulated jumps were based (see Fig. 4B) are given in the first row; beta angle could not be measured from the video images. Characteristics of the simulated jumps are given in subsequent rows; procedures for calculating them are given in the Materials and methods. In those *jumps*, either no *dorsiflexion* stimulus current was applied, or the stimulus current ramp amplitude varied from 17.5 to 19 nA. *Beta angle* was set to the take-off angle measured from the live locust, and the *initial pitch* was adjusted (see Materials and methods) to be near the value from the real animal.

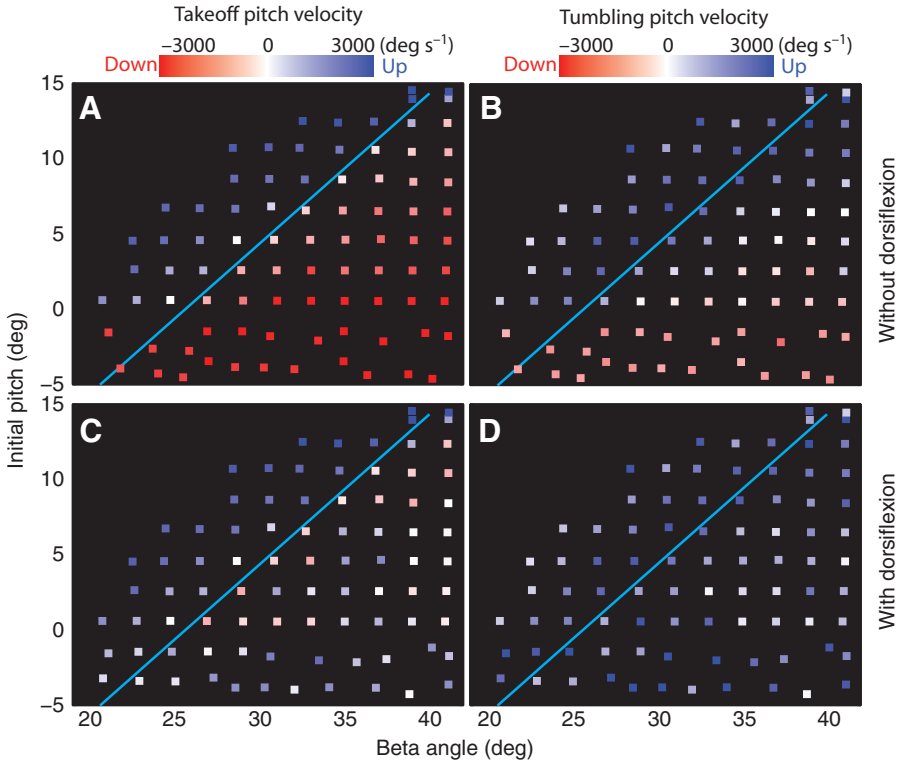

Fig. 8. Relationship of the *take-off* and *tumbling pitch velocities* to the *initial pitch* and *beta angle* for simulated jumps. Locust jumps were simulated without (A and B) and with (C and D) *dorsiflexion*. *Take-off pitch velocities* (*TOPV*, left panels in A and C) and *tumbling pitch velocities* (*TUPV*, right panels in B and D) are color coded, with more red squares marking *jumps* with negative (head-downward) *pitch velocities*, and more blue squares marking *jumps* with positive (head-upward) *pitch velocities*. The cyan lines in all four plots are the regression lines of the initial pitch *vs* take-off angle for the jumps of locust 2 (Fig. 4B).

occurred at *take-off* (Fig. 8A,C), and along a series of *jumps* for which low head-upward *tumbling* occurred after *take-off* (Fig. 8B,D). The agreement between the behavior of locust 2 and its model suggests that dorsiflexion and the variation of initial pitch with beta angle are mechanisms used by the locust to control tumbling.

As was described above, greater abdominal flexion occurred for most live jumps when the take-off pitch velocity was more negative (Fig. 5A); head-downward tumbling was then effectively eliminated or reversed (Fig. 5B). To test whether a similar variation in *abdominal flexion* of the locust model would have the same effect on *tumbling* for a range of initial *pitches* and *take-off pitch velocities*, larger and smaller currents were applied to the *dorsal longitudinal motor neuron* for *locust jumps* that began from different initial *body* pitches (Fig. 5C,D). These simulations showed that more *dorsal longitudinal muscle* activation was required to reverse the greater downward *take-off pitch velocity* produced by a smaller initial *body pitch*. An initial *body pitch* of 5 deg and a *motor neuron* stimulus current of 8 nA produced *abdominal flexions* between 15 deg and 32 deg and *TOPVs* between –400 deg s^{-1} and –1300 deg s^{-1} (Fig. 5C, red); these led to *TUPV* values between –400 deg s^{-1} and 2200 deg s^{-1} (Fig. 5D, red). Similar positive shifts in *pitch velocity* occurred when the initial *body pitch* was greater, and smaller stimulus currents evoked correspondingly smaller *abdominal flexions* (Fig. 5C,D, green, blue). Negative *torque* for these simulated *jumps* was greatest when the *initial body pitch* was low, and so greater *dorsal longitudinal muscle* activation was required to produce a *counter-torque* that would eliminate or reverse the head-downward *tumbling*. The simulations reproduce the responses of the animals as they jumped with varying TOPVs and degrees of dorsiflexion (Fig. 4; Fig. 5A,B), suggesting that the same mechanisms are at work in both the live animals and simulations. As was seen in the live animals the TUPV was parallel to and shifted right from the corresponding plots of abdominal flexion *vs* TOPV for the simulation (2203±617 deg s^{-1}).

Relationship between beta angle and take-off angle

An earlier analysis of locust jumping (Sutton and Burrows, 2008) showed that the beta angle, formed by a line between the tarsus and femur–tibial joint and the horizontal plane, defines the thrust vector of the jump. If the thrust vector passes through the COM projected onto the plane of the leg, then the jump will follow the thrust vector and the take-off angle will equal the beta angle. If, however, the COM is off the thrust vector, then the reaction to torque around the COM will tend to push the femur–tibial joint in the opposite direction, and thereby change the direction of the thrust vector. This conclusion was examined by plotting the *take-off vs beta angle* for a set of simulated *jumps* with different initial *pitches* and *beta angles*

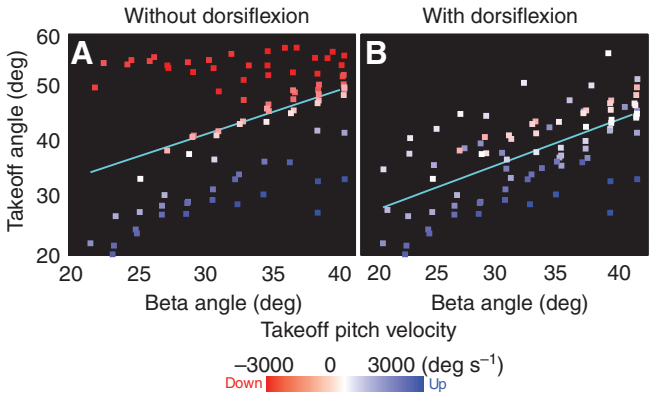

Fig. 9. Effect of *dorsiflexion* on *take-off angle* in simulated *jumps*. (A) *Take-off angles* for *jumps* at different *beta angles* and without *dorsiflexion*. The regression line (cyan) on all points has a slope/intercept of 0.93/14.4 deg (R^2=0.17). (B) *Take-off angles* for *jumps* with *dorsiflexion* (average stimulus current=32.6±13 nA). *Take-off velocities* varied approximately linearly with *beta angle*. The regression line (cyan) on all points has a slope/intercept of 1.05/4.04 deg (R^2=0.43).

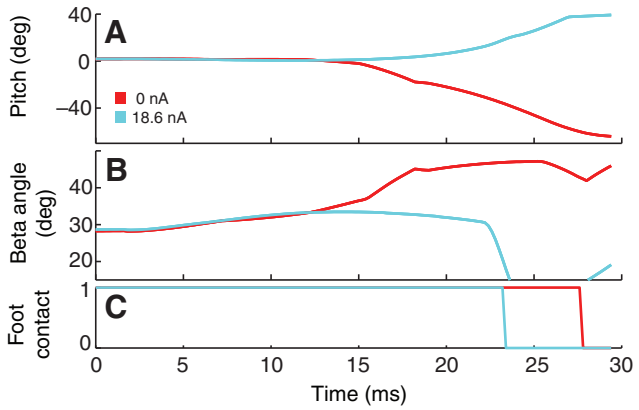

Fig. 10. *Beta angle* shifts without *dorsiflexion*. Simulations were the same as in Fig. 6. The *pitch* (A) and *beta angle* (B) remained constant before take-off (C) when a *dorsiflexion* (cyan) was present, but *pitch* decreased and *beta angle* increased without *dorsiflexion* (red).

(Fig. 9A). *Jumps* with large head-downward *TOPV* were strongly skewed towards a *take-off angle* of 60 deg, and the closer the velocity was to zero, the less the *take-off angle* was skewed. *Jumps* with a head-upward *TOPV* tended to have low *take-off angles*. When *dorsiflexions* were stimulated during the *jumps*, a more linear relationship between *beta angle* and *take-off angle* occurred with a slope/intercept of 1.05/4.04 deg and correlation coefficient R^2=0.43 (Fig. 9B).

The *beta angle* was initially the same in simulations with and without a *dorsiflexion*, and then diverged about half-way to *take-off*. When no *dorsiflexion* occurred, negative torque around the *COM* caused the *body* to pitch head-downward (Fig. 10A) and the *beta angle* to increase sharply to over 50 deg (Fig. 10B). *Dorsiflexion* caused the *body pitch* to increase more slowly upward as the *beta angle* (and the resulting thrust direction) remained constant until the *feet* left the ground (Fig. 10).

DISCUSSION

We found that locusts' take-off angles varied in proportion to their initial body pitch prior to jumping (Fig. 4). For locust 2, this relationship minimized tumbling over a large range of take-off angles. Simulations of locust jumping demonstrated that the initial body pitch adopted by live locusts at each beta angle were close to the optimum value that minimized *tumbling* for the model *locust*. This suggests that control of tumbling is important during locust jumping, and supports the hypothesis that the locust deliberately adopts a posture for a given take-off angle that will keep the tumbling velocity low. By changing the initial body pitch, a locust can move its COM closer to the intended thrust vector, and so reduce the torques acting on the body during the jump impulse.

Contraction of the abdominal muscles prior to and during the jump impulse could function as a secondary mechanism to control tumbling. Simulations where the *DLM* was contracted in this manner were able to recreate results very similar to the behavior of the real locust, and when that contraction was absent it behaved in a predictable manner, but one that was never seen in real locust jumps. Varying the magnitude of the contraction also allowed the *take-off pitch velocity* to be controlled and made it possible to convert all of the simulated *jumps* with head-downward *TUPV* into head-upward velocities. As with the live locusts, this mechanism allowed the simulated *locust* to always have a head-upward *TUPV* regardless of the *initial pitch* or *beta angle* that was adopted for the *locust*.

This implies that as a locust adjusts its pitch prior to jumping, it must also estimate the amount of dorsiflexion that will be needed. This is further supported by the rate of the jump, which occurred over a span of 20–35 ms, with the bulk of the acceleration occurring in the last 10–15 ms (Bennet-Clark, 1975; Brown, 1967). The speed of the jump makes it unlikely that a reflex circuit alone could be responsible for controlling the dorsiflexion. However, it is possible that a reflex circuit assists an already active dorsiflexion when a downward TOPV causes the dorsal abdominal muscles to stretch.

Data from the high-speed video also suggests that there is a bias in the way locusts use abdominal muscles during control of tumbling. Very few abdominal ventral flexions were seen for the live animals, and the few that were visible had a much smaller magnitude than the dorsiflexions. Simulations of ventral extensions were effective in reducing the *pitch velocities* for postures that produced a *jump* that pitched rapidly head-upward (not shown). Locusts could use ventral flexions to control head-upward tumbling similar to the way that dorsiflexions control head-downward tumbling, but the locusts do not do this; head-downward tumbling was corrected, but head-upward tumbling was not.

Indeed, in our experiments, locusts rarely displayed head-downward tumbling pitch velocities. Regardless of the initial pitch or the beta angle adopted by locust 2, it always had a head-upward pitch velocity, and only 5 of 126 jumps from all locusts tested had head-downward velocities. This bias may be due to an evolutionary advantage related to flight. Locusts typically initiate flight by jumping (Bicker and Pearson, 1983; Pond, 1972). A locust jumping at a positive angle with respect to the horizon would experience lift if it spread its wings, whereas when its posture was negative it would be driven back to the ground, which would prove disastrous when attempting to escape a predator. From an evolutionary perspective, therefore, it makes more sense for the locust to pitch up instead of down. So although using the ventral abdominal muscles could potentially reduce head-upward tumbling pitch velocities, it may make it more likely that a head-upward tumble would be converted into being head-downward, and that could have potentially fatal consequences.

A key assumption in the previous work that related beta angle to the control of jump elevation was that the COM was located directly at the site of force application (Sutton and Burrows, 2008). The COM is so close to the CF joint that this was a justifiable simplification of the model that greatly reduced the mathematical complexity. However, the COM is not actually located there, so that the COM can be out of the line of the thrust vector and lead to torques that produce tumbling. By altering its body pitch prior to jumping, the locust can minimize this error. We have shown that when the *take-off pitch velocity* of the *locust* was close to zero, the *beta angle* was a good predictor of the *take-off angle*, and that they varied in linear fashion with a slope of one. When the *velocity* became strongly head-downward, as happens without *dorsiflexions*, the *beta angle* shifted during the *jump* as the *body* rotated forward, and this skewed the *thrust* and the *take-off angle* upwards. So it appears that control of tumbling is not only important for maintaining the orientation of the body during the jump, but also for ensuring that the thrust vector remains constant.

It is unclear whether the mechanisms outlined here will be generally applicable to other jumping animals. For instance, while the bush cricket (*Pholidoptera griseoptera*) has a number of differences in its jumping mechanism compared with the locust, it shares enough similarities that one would expect it to face similar challenges regarding control of tumbling. However, recordings of their jumping failed to find examples of tumbling (Burrows and Morris, 2003). This suggests that its COM is directly located at the point of

thrust application. Other animals such as the flee-beetle (Alticinae) appear to use their wings to prevent tumbling (Brackenbury and Wang, 1995). This differs from locusts in that flee-beetles typically open their wings before take-off, while locusts open their wings 20–30 ms after the tarsi have left the ground (Pond, 1972).

Neuromechanical simulation allowed us to rapidly test alternative hypotheses on the control of tumbling and find two mechanisms that were able to closely reproduce results from live animals. However, it will still be necessary to test the role of abdominal muscles in live animals. This could be done by recording EMGs of abdominal muscles before and during the jump, or by paralyzing or cutting abdominal muscles to see the results on tumbling.

LIST OF ABBREVIATIONS

CF	coxo-femoral joint
COM	center of mass
DLM	dorsal longitudinal muscle
FT	femoro-tibial joint
TOPV	take-off pitch velocity
TUPV	tumbling pitch velocity
β	beta angle

ACKNOWLEDGEMENTS

We wish to acknowledge support for this work from National Science Foundation research grant 0641326 to D.H.E.; from a Brains & Behavior Seed Grant from Georgia State University, from the Brains & Behavior Fellowship Program at Georgia State University, and from National Institutes of Health exploratory grant GM065762. We would also like to thank Dr Karen Thompson of Agnes Scott College for supplying us with locusts for testing, and for instructing us on their maintenance and care. Deposited in PMC for release after 12 months.

REFERENCES

Albrecht, F. O. (1953). *The Anatomy of the Migratory Locust*. London: The Athlone Press.
Alexander, R. M. (1968). *Animal Mechanics*. Seattle: University of Washington Press.
Baader, A. (1990). The posture of the abdomen during locust flight. Regulation of steering and ventilatory interneurones. *J. Exp. Biol.* **151**, 109-131.
Bennet-Clark, H. C. (1975). The energetics of the jump of the locust Schistocerca gregaria. *J. Exp. Biol.* **63**, 53-83.
Bicker, G. and Pearson, K. (1983). Initiation of flight by an identified wind sensitive neurone (TCG) in the locust. *J. Exp. Biol.* **104**, 289-293.
Brackenbury, J. and Wang, R. (1995). Ballistics and visual targeting in flea-beetles (Alticinae). *J. Exp. Biol.* **198**, 1931-1942.
Brown, R. H. J. (1967). The mechanism of locust jumping. *Nature* **214**, 939.
Burrows, M. (1995). Motor patterns during kicking movements in the locust. *J. Comp. Physiol. A* **176**, 289-305.
Burrows, M. (1996). *The Neurobiology of an Insect Brain*. Oxford: Oxford University Press.
Burrows, M. and Morris, G. (2001). The kinematics and neural control of high-speed kicking movements in the locust. *J. Exp. Biol.* **204**, 3471-3481.
Burrows, M. and Morris, O. (2003). Jumping and kicking in bush crickets. *J. Exp. Biol.* **206**, 1035-1049.
Camhi, J. M. (1970a). Sensory control of abdominal posture in flying locusts. *J. Exp. Biol.* **52**, 533-537.
Camhi, J. M. (1970b). Yaw-correcting postural changes in locust. *J. Exp. Biol.* **52**, 519-531.
Cofer, D., Cymbalyuk, G., Reid, J., Zhu, Y., Heitler, W. and Edwards, D. H. (2010a). AnimatLab: a 3-D graphics environment for neuromechanical simulations. *J. Neurosci. Methods* **187**, 280-288.
Cofer, D. W., Cymbalyuk, G., Heitler, W. J. and Edwards, D. H. (2010b). Neuromechanical simulation of the locust jump. *J. Exp. Biol.* **213**, 1060-1068.
Eriksson, E. (1980). Movement Parallax and distance perception in the grasshopper (*Phaulacridium vittatum*). *J. Exp. Biol.* **86**, 337-340.
Gettrup, E. and Wilson, D. M. (1964). The lift-control reaction of flying locusts. *J. Exp. Biol.* **41**, 183-190.
Heitler, W. (1974). The locust jump. Specialisations of the metathoracic femoral-tibia joint. *J. Comp. Physiol.* **89**, 93-104.
Heitler, W. J. and Burrows, M. (1977). The locust jump. I. The motor programme. *J. Exp. Biol.* **66**, 203-219.
Hill, A. V. (1970). *First and Last Experiments in Muscle Mechanics*. Cambridge: Cambridge University Press.
Pearson, K. G., Heitler, W. J. and Steeves, J. D. (1980). Triggering of locust jump by multimodal inhibitory interneurons. *J. Neurophysiol.* **43**, 257-278.
Pond, C. (1972). The initiation of flight in unrestrained locust *Schistocerca gregaria*. *J. Comp. Physiol.* **80**, 163-178.
Santer, R. D., Yamawaki, Y., Rind, F. C. and Simmons, P. J. (2005). Motor activity and trajectory control during escape jumping in the locust *Locusta migratoria*. *J. Comp. Physiol. A* **191**, 965-975.
Shadmehr, R. and Wise, S. (2005). *Computational Neurobiology of Reaching and Pointing: a Foundation for Motor Learning*. Cambridge, MA: MIT Press.
Sobel, E. C. (1990). The locust's use of motion parallax to measure distance. *J. Comp. Physiol.* **167**, 579-588.
Sutton, G. P. and Burrows, M. (2008). The mechanics of elevation control in locust jumping. *J. Comp. Physiol. A* **194**, 557-563.